

EXPERIMENTAL AND NUMERICAL DESIGN AND CHARACTERISATION OF A SUPERSONIC IDEAL NOZZLE FOR FREE-JET TEST FACILITIES

Berk Bozkır¹, M. Tuğrul Akpolat², Ezgi Arısoy³ and I. Taylan Karpuzcu⁴
ROKETSAN Missiles Inc.
Ankara, Turkey

ABSTRACT

Within the concept of this paper, design of a supersonic ideal nozzle is conducted employing Method of Characteristics (MOC). Then, in order to validate the results of MOC, an experimental campaign is performed using an instrumented nozzle with pressure taps together with the numerical investigation using Computational Fluid Dynamics (CFD) method. MOC and CFD results are obtained to be in good agreement with the experimental results. Nevertheless, at the near-exit locations, a slight deviation between the results is observed due to relatively thicker boundary layer through the nozzle-exit and to the fact that MOC method has an inviscid approach. In addition, the experimental setup has immeasurable swirl pattern based on its design, which also has an effect on this slight variation between the experimental and MOC as well as the CFD results. Moreover, flow separation is observed for the pressure ratio (PR) values of below 6 along with its movement through the nozzle throat by lowering the PR value.

INTRODUCTION

Supersonic ideal nozzles are employed for high-speed aircrafts and missiles in order to convert the pressure energy to kinetic energy. Another use of supersonic ideal nozzles is free-jet test facilities. In free-jet test facilities, supersonic ideal nozzles are used to maintain the flow conditions for a supersonic test article. Therefore, characterization and evaluation of ideal nozzles are of high importance for the design of exhaust nozzles of supersonic aircraft and missiles, as well as free-jet test facilities. This can be conducted by employing the Method of Characteristics (MOC) or the Computational Fluid Dynamics (CFD) methods however; both the MOC and the CFD methods should be validated by conducting various experiments.

MOC is a well-known, simple and efficient method for the design of inviscid supersonic nozzles. MOC is used for solving the nonlinear differential equation for the velocity potential which expresses a two dimensional, steady, isentropic, irrotational flow. By employing MOC, the governing partial differential equations are converted into ordinary differential equations. When the equations become hyperbolic, method of characteristics can be used to solve them. A characteristic is a line that the information propagates and for the supersonic flow in consideration it is called the Mach lines. The method uses a starting sonic line from the throat of the nozzle as the initial guess and then solves the Euler equations. For each point whose

¹ Engineer at Propulsion System Design Department, Email: berk.bozkir@roketan.com.tr

² Specialist Engineer at Propulsion System Design Department, Email: tugrul.akpolat@roketan.com.tr

³ Specialist Engineer at Propulsion System Design Department, Email: ezgi.arisoy@roketan.com.tr

⁴ Engineer at Propulsion System Design Department, Email: taylan.karpuzcu@roketan.com.tr

properties such as Mach number, velocity vector, temperature etc. are known through the line. Two characteristic lines are introduced from this point and at the intersections of these characteristic lines that are coming from other points, a new solution point is created. Repeatedly solving these lines a web of points is created and the flow field is solved.

Experimental studies may be used to validate the results obtained by the MOC or the CFD methods. Since they are expensive, the use of experimental techniques alone as a nozzle design tool is not advisable. For supersonic ideal nozzles; flow visualization techniques such as Schlieren at the exit of the nozzle, pressure and temperature measurements from the walls of the nozzle etc. are widely used experimental characterization techniques as an evaluation of the nozzle performance as well as a validation.

Murugan [Murugan, 2003] employed MOC as a design methodology for a scramjet nozzle. The results showed good agreement with the results from literature and that of an Euler solver. Seckin [Seckin, 2003] used MOC in order to design an ideal nozzle contour and compared the results with the test cases. A thorough review on the nozzle flow separation phenomenon is presented by Hadjaj and Onofri [Hadjaj & Onofri, 2009]. Verma [Verma & Haidn, 2007] studied the nozzle flow separation experimentally employing wall pressure measurements and color Schlieren flow visualization with the focus on the side-load in a truncated ideal nozzle. The results indicated that the side-load is mostly caused by the fluctuations of the separation shock in the separated region.

EXPERIMENTAL SETUP

In order for the validations, the experiments are carried out at the Connected Pipe Test Facility. The facility consists of the high-pressure air storage tanks, pressure control valves and an air vitiator. For the purposes of this study, the nozzle is fitted at the exit of the air vitiator, without the vitiator, i.e. with cold air flow. In order to provide the required pressure ratios (PR) between the inlet and the exit of the nozzle the pressure at the inlet of the nozzle is regulated by the control valves. A basic scheme of the test setup is represented in Figure 1.

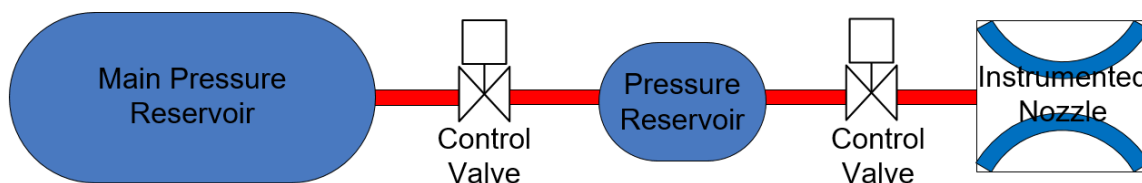


Figure 1: Schematic of the test setup

This nozzle is designed by using the in-house developed MOC code by Seçkin (2003). The resulting contour of this code ensures that the flow is uniform at the exit section of the nozzle. The code works by the following procedure:

- Flow field in the throat region is determined (sonic line)
- An initial value line is determined using the throat region solution
- A Kernel point where the target Mach number is calculated and a line connecting this point with the exit section diameter point that is calculated from the mass conservation is created.
- By using this Kernel line as the starting point, equations are solved to the wall by utilizing the two characteristic lines that goes out from each point.

- The wall contour is determined by using the angles of the characteristic lines with x axis. When the flow angle and the characteristic line angle equalized, the point on the wall is determined.

The inputs to the code are the fluid variables, throat diameter, exit Mach number and number of points of the starting line.

The nozzle used for the experiments is so-called an axisymmetric instrumented nozzle, which has 18 pressure tapping throughout its outer wall in order to conduct pressure measurements. The distribution of the pressure taps along with the upstream pressure measurement tap (for total pressure) are as shown in Figure 2. The instrumented nozzle to be used, shown in Figure 2, has the inlet diameter of 324 mm, the throat diameter of 64.51 mm and the exit diameter of 103 mm.

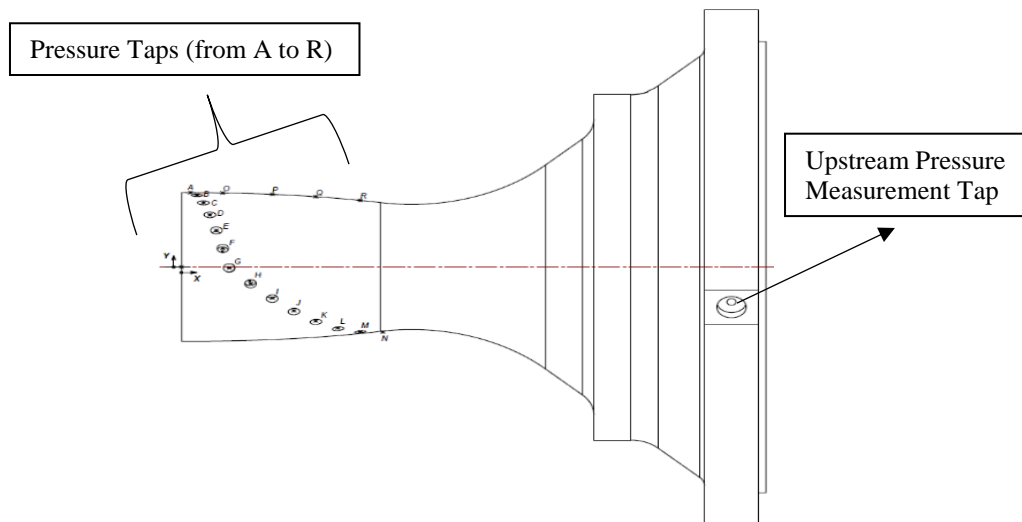


Figure 2: Axisymmetric instrumented nozzle along with the pressure taps

The pressure measurements are performed by using a NetScanner 9116 pressure scanner, consisting of 16 pressure channels. Since the instrumented nozzle has 18 pressure taps, 2 of them were blanked. The pressure tapping are connected to the pressure channels by Teflon hoses of 1/8" diameter. The upstream total pressure at the inlet of the nozzle is measured using a Keller pressure sensor.

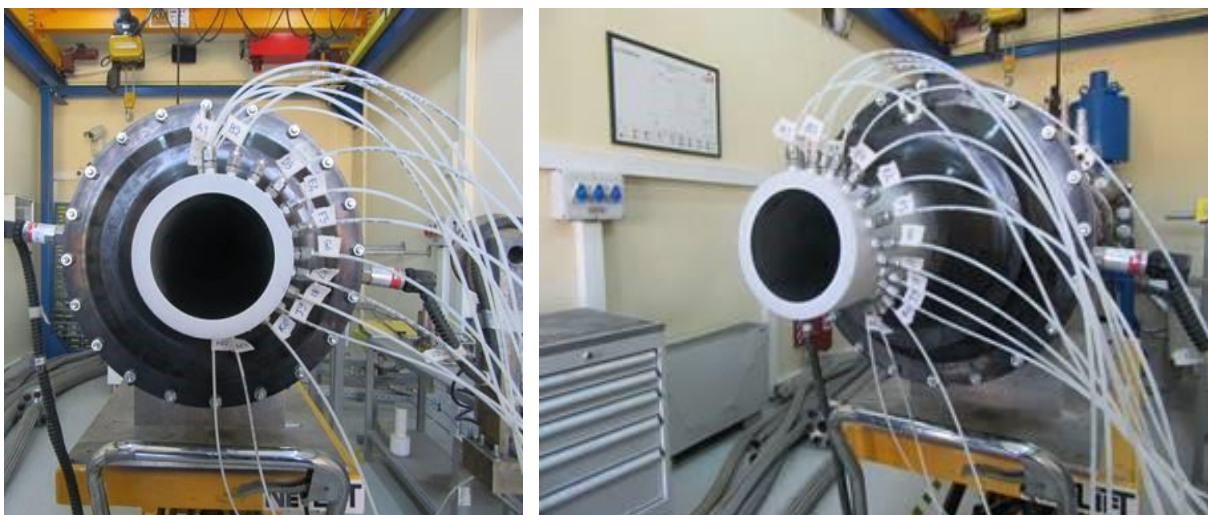


Figure 3: Instrumented nozzle with hoses inserted to the pressure taps

RESULTS

The ratio of total pressure of the flow to the atmospheric pressure (PR) throughout the experiment is presented in Figure 4. The reason the PR plot behaves to be oscillatory is the flow being manually controlled by two control valves behind the instrumented nozzle and the pressure reservoir between two control valves and the upstream main reservoir is varying.

In addition, the total pressure of the flow is a function of the upstream pressure of the control valves as well as the percentage opening of the valves themselves. Therefore, a wide range of pressure ratios (PR) can be evaluated as each discrete time represents a PR value which results the measurements up to ~ 12 as can clearly be observed from Figure 4.

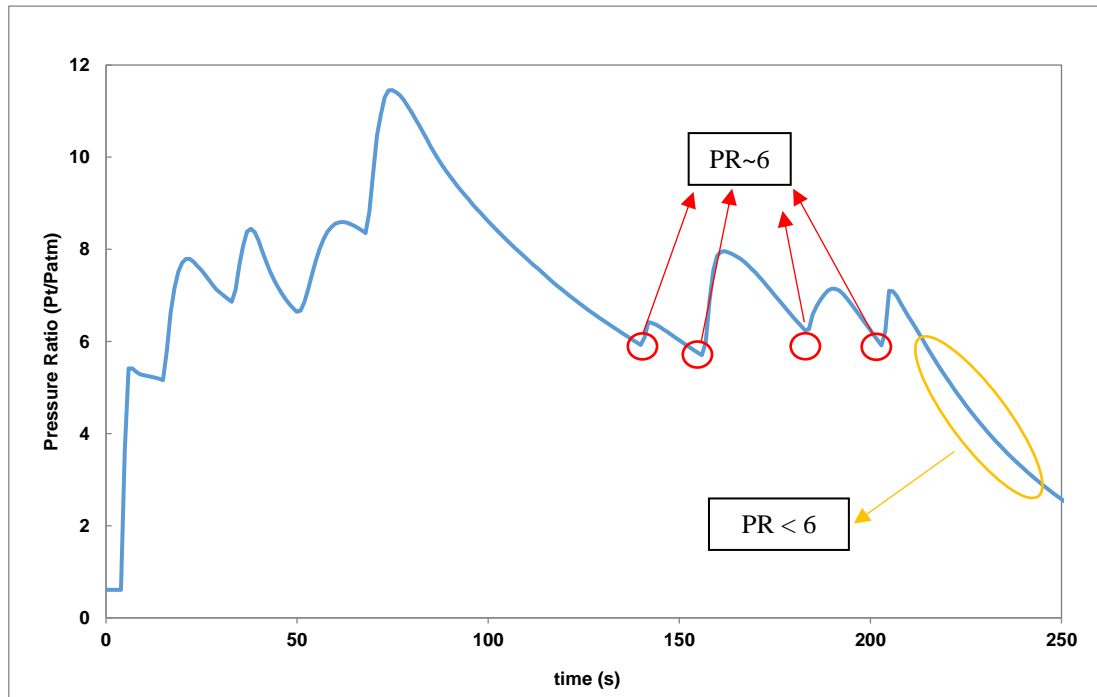


Figure 4: The ratio of the total pressure to the exit (atmospheric) pressure (PR)

Figure 5 indicates the ratio of the wall static pressures at all pressure taps to the total pressure of the flow (P/P_t) for all of the pressure taps located from nozzle throat to nozzle exit. Higher PR valued measurements refer to locations through the nozzle throat whereas lower ones refer to location through the nozzle exit at each distinct time along the experiment.

As can be seen in the figure, as PR drops approximately below ~ 6 , flow separates from the nearest pressure tap position to the exit. These abrupt pressure changes from the near-exit pressure tap can be observed at $t \sim 130$ s, $t \sim 140$ s, $t \sim 175$ s, $t \sim 195$ s and $t \sim 215$ s indicated both in Figure 4 and Figure 5.

For the PR values lower than ~ 6 , remaining channels corresponding to the location from the nozzle exit through the nozzle throat, consecutive pressure jumps representing the separation movement through the nozzle throat can be observed following the $t \sim 215$ given in Figure 5.

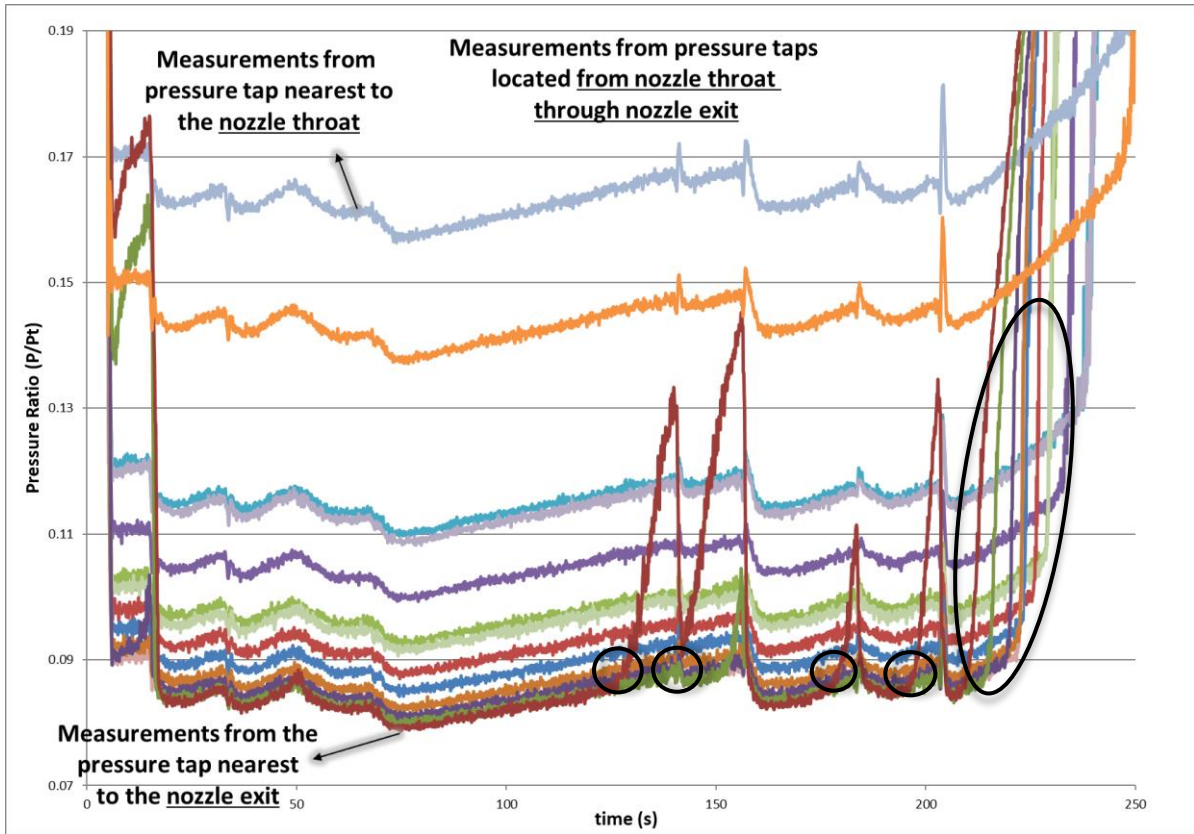


Figure 5: Measurements from the pressure taps from nozzle throat (highest static to total pressure ratio – P/Pt) through the nozzle exit (lowest static to total pressure ratio – P/Pt) (PR ~ 6 and PR > 6 regions where separation is observed are marked)

In addition, a separate plot also showing the tap at the nearest location to the nozzle exit and the PR, is given in Figure 6, indicates flow the separated flow for PR values below ~6 starting from the pressure tap located very next to the nozzle exit.

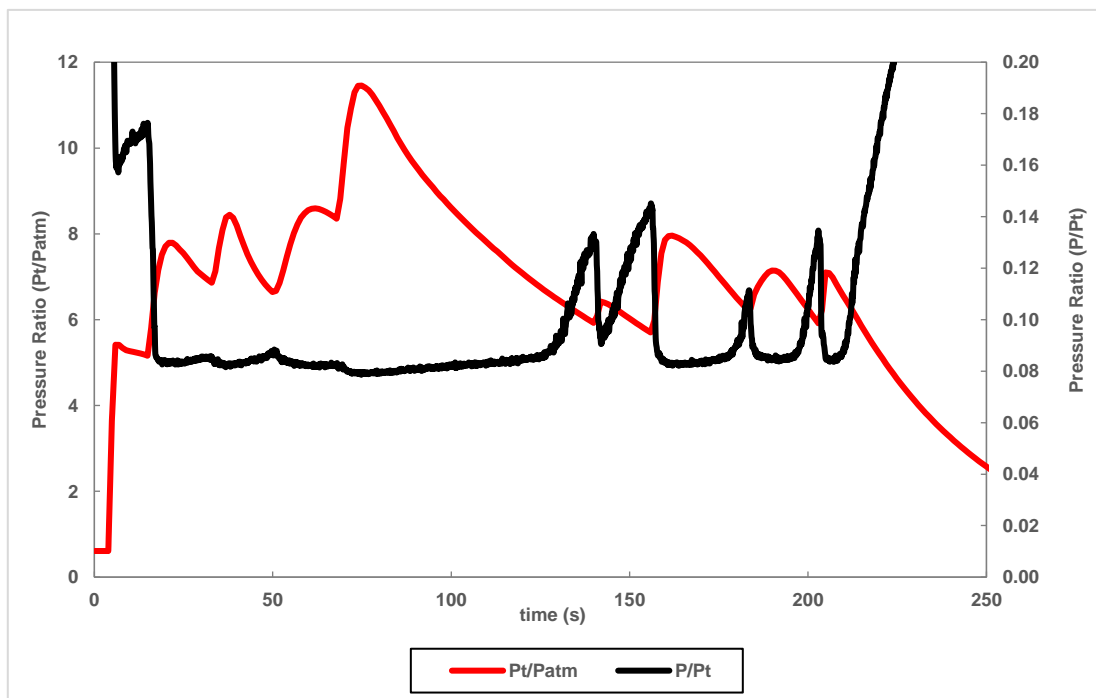


Figure 6: Measurements from the pressure tap nearest to the nozzle exit

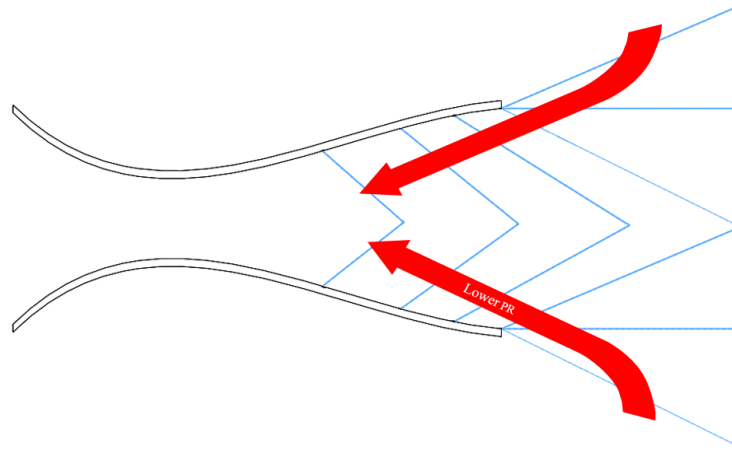


Figure 7: Example flow patterns and visualizations with lowering the PR values

The behavior of the pressure jumps mentioned previously is visualized in Figure 7. The blue lines represent the sonic line for individual values of PR and as PR degrades, the sonic region starts to shrink through the nozzle throat. This movement arises with a separation primarily from the very exit of the nozzle and can be observed from a pressure measurements acquired at the wall. For the case, $PR \sim 6$ can be said to be the critical value and represents the point where further lowering the PR causes the flow to separate therefore the jumps in the pressure measurements.

Moreover, a Computational Fluid Dynamics (CFD) simulation is performed in order to further reveal the flow behavior through the objective instrumented nozzle. A case where no flow separation is expected to occur is examined in order to compare the MOC results and experimental measurements given in with the wall pressures acquired from the CFD study. Besides, a case where flow separation arises starting from nozzle exit through the throat is investigated and the consistency of the results is evaluated. For the CFD simulations, a well-known commercial FloEFD code is used. Priorly, a grid convergence study is performed and the grid size of 5 million (quarter-symmetrical domain) cells including the local refinements is obtained to be the sweet-spot for the calculations where further grid refinement would not worth the cost.

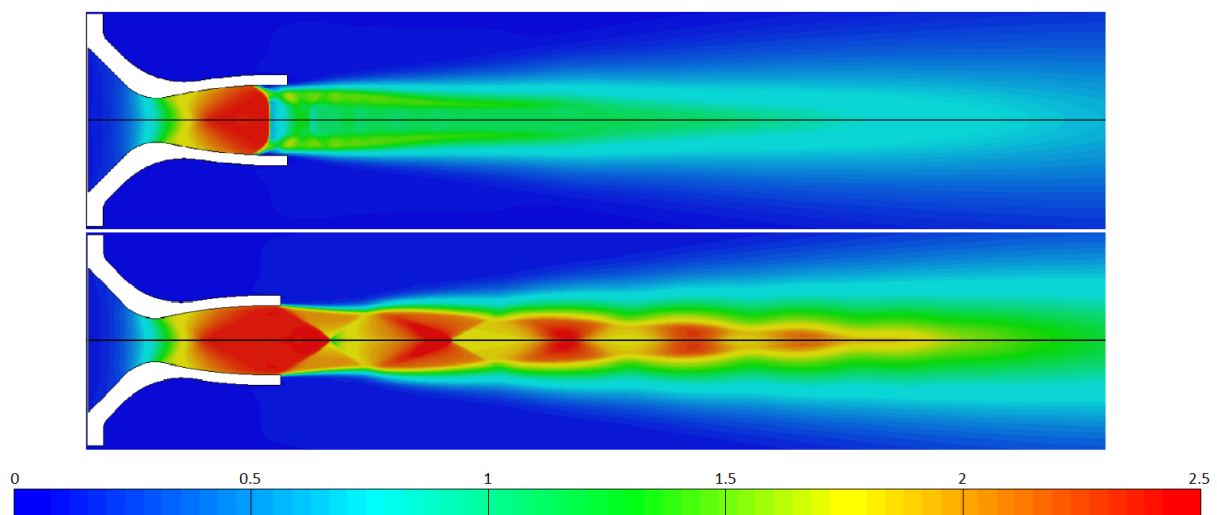


Figure 8: Mach contours for $PR=4$ (upper) and $PR=10$ (lower)

Pressure contours of $PR=4$ and $PR=10$ is given in Figure 8. As stated, for $PR=10$ case represents the flow without separation whereas the case of $PR=4$ is selected to demonstrate the flow separation observed through the experiment. Figure 8 represents the comparison between the flow with and without a separation and as it can be observed, the case with PR value of 4 results a flow separation located a certain distance upstream of the nozzle exit whereas for $PR=10$, no separation can be spotted.

The experimental and CFD results as well as the results from the MOC calculations for the static to total pressure ratio (P/P_t) vs. the distance from throat normalized with the throat diameter is as shown in Figure 9. Moreover, the case of $PR>6$ ($PR=10$) where no flow separation is expected to occur is investigated in order to compare the MOC results and experimental measurements with the numerical wall pressures acquired from the CFD simulation given in Figure 9.

The first experimental data points are in good agreement between the MOC and CFD calculations given in Figure 9. However, through the near-exit locations of the nozzle the experimental results start to differ. This is caused by the relatively thicker boundary layer at the exit of the nozzle. Since the boundary layer is thicker, the inviscid results of the MOC starts to vary slightly. In addition, the flow at the upstream of the nozzle has an immeasurable swirling pattern due to the design of the test setup itself. As this swirl cannot be implemented as a boundary condition for the CFD simulation, the experimental results have slight diversity from the MOC and CFD results.

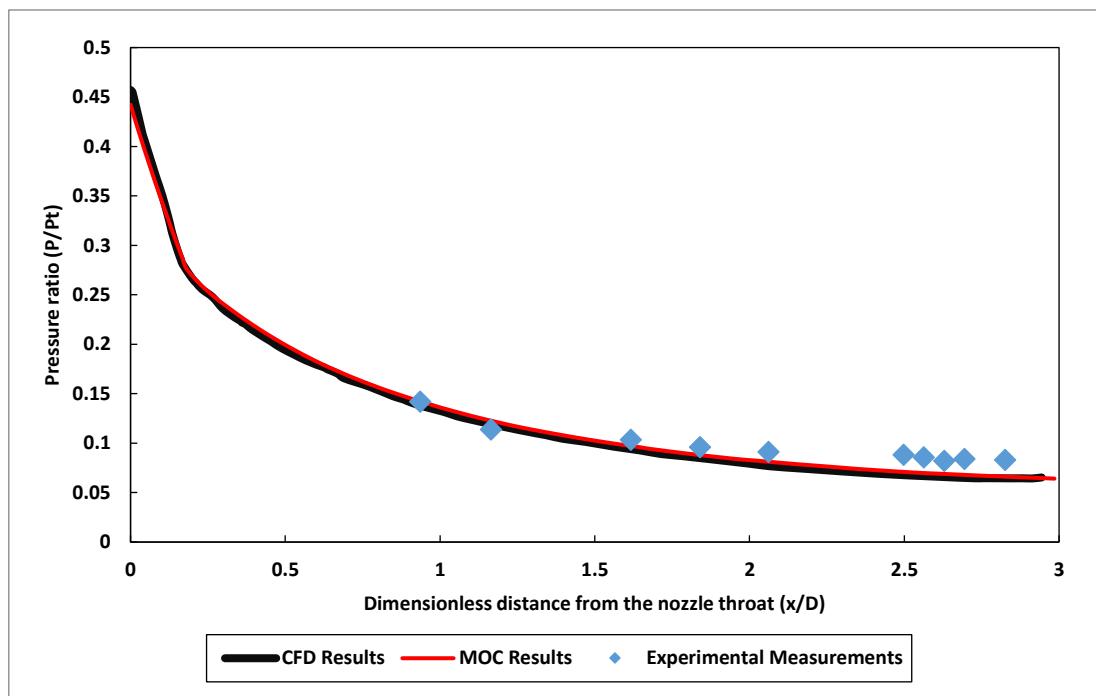


Figure 9: Comparison of wall pressures for CFD, MOC and experimental results of $PR>6$

In addition, pressure ratio values of experimental measurements as well as the CFD simulation is presented in Figure 10 for $PR=4$ where flow separation is expected to arise. Similarly, the pressure ratio values are introduced as a function of dimensionless distance from the nozzle throat within the plot. It is observed that the location of the separation is slightly upstream of what CFD results denote, presumably due to the immeasurable swirling pattern as mentioned and the ability of the solver on capturing the phenomena. However, the overall trend is very-well obtained and the pressure measurements downstream of the separation (last five tap locations through the nozzle exit) match almost perfectly with the CFD results.

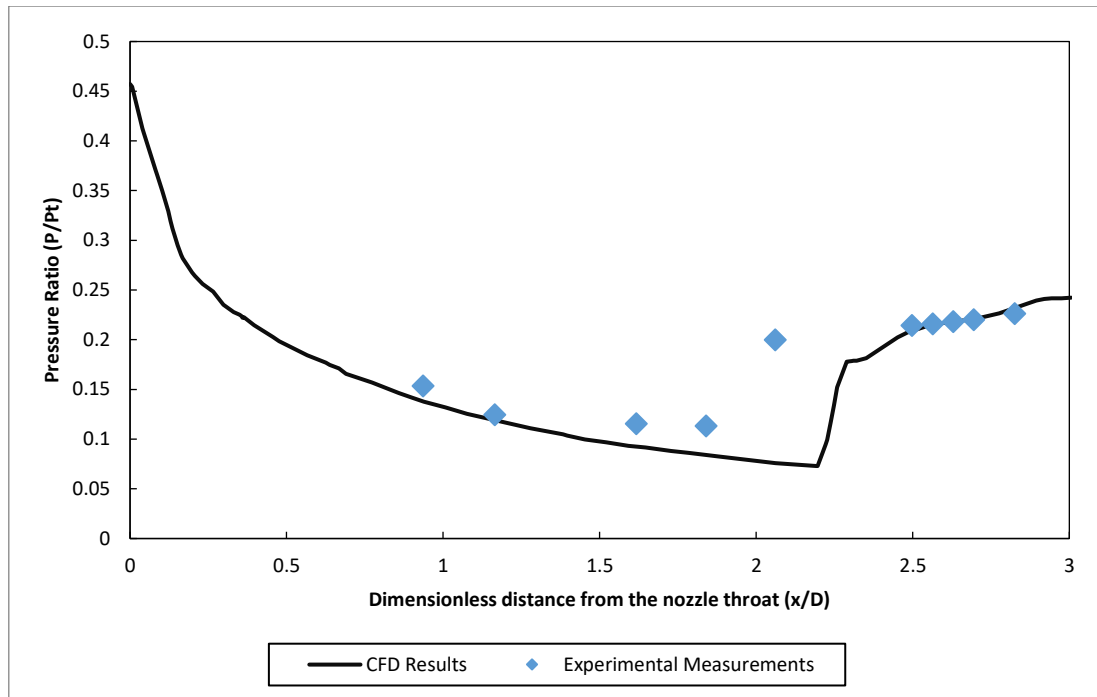


Figure 10: Comparison of wall pressures for CFD and experimental results of PR=4

CONCLUSION

Within the scope of this study, an experimental campaign using an instrumented nozzle, with pressure taps located all along the diverging section, was conducted. The flow separation at the near-exit locations of the nozzle for PR values lower than ~6 is well-documented with the experimental results along with the movement resulted by further lowering PR. Then, the experimental results were compared with results obtained by the MOC method as well as the CFD simulation. Both the MOC and CFD results indicated a good agreement with the experimental results at the near-throat positions of the nozzle. However, at the near-exit positions, the results were started to drift away from each other. Since the MOC method gives an inviscid solution and the flow at the vicinity of the nozzle exit is mostly dominated by relatively thicker boundary layer, this variation can be evaluated as acceptable. In addition, the flow at the upstream of the nozzle has an immeasurable swirling pattern due to the design of the test setup itself, which can neither be implemented to MOC nor to CFD study. This swirl also has an effect on this slight diversity of the pressure measurements from both the MOC and the CFD results, as presented within the paper.

References

- Hadjadj, A., & Onofri, M. (2009). Nozzle Flow Separation. *Shock Waves*, 19, 163-169. doi:10.1007/s00193-009-0209-7
- Murugan, T. (2003). *Scramjet Nozzle Design Using Method of Characteristics*. Kanpur, India: M.Sc. Thesis.
- Seckin, B. (2003). *Rocket Nozzle Design and Optimization*. Ankara, Turkey: M.Sc. Thesis.
- Verma, S., & Haidn, O. (2007). Flow Separation Studies in a Subscale Truncated Ideal Contour Nozzle. *45th AIAA Aerospace Sciences Meeting and Exhibit*. Reno, Nevada: AIAA 2007-1320.